

## **Fabrication of Nb-SIS mixers with UHV evaporated Al striplines**

J.R. Gao<sup>+#</sup>, S. Kovtonyuk<sup>1+</sup>, J.B.M. Jegers<sup>+</sup>, P. Dieleman<sup>+</sup>, T.M. Klapwijk<sup>+</sup>, and  
H. van de Stadt<sup>#</sup>

<sup>+</sup> Department of Applied Physics and Materials Science Center, University of Groningen,  
Nijenborgh 4, 9747 AG Groningen, The Netherlands

<sup>#</sup> Space Research Organization of the Netherlands, PO Box 800, 9700 AV Groningen  
The Netherlands

### **Abstract**

We have succeeded in developing a novel fabrication process for Nb SIS junctions integrated with an aluminium (Al) stripline for 1 THz waveguide mixers. In particular, a pure Al film, which is evaporated in an ultra-high vacuum system, is applied for the stripline. It can provide a lower surface resistance in comparison with a sputtered Al film, consequently reducing radio frequency (RF) loss in the tuning element. The junctions are fabricated with standard photolithography and typical junction areas are  $1 \mu\text{m}^2$ . The heterodyne measurements performed at a temperature of  $\geq 4.2$  K show that high frequency video response extends up to 1.1 THz and the best DSB noise temperatures are 700 K at 900 GHz and 1000 K at 1 THz.

---

<sup>1</sup> Permanent address: Institute for Radio Engineering and Electronics, Russian Academy of Sciences, Mochoyova str. 11, Moskow 103907, Russia.

## I. Introduction

It has been demonstrated by several research groups that up to the gap frequency of 700 GHz Nb-SIS junctions with integrated tuning elements can provide sensitive heterodyne detection near the quantum noise limit. A traditional tuning element consists of a superconducting stripline, Nb/SiO<sub>x</sub>/Nb sandwich structure. At high frequencies this element is essential to efficiently couple a RF signal to a Nb SIS junction. In a well designed superconducting tuning circuit, RF losses are usually negligibly low. As the frequency extends beyond the gap frequency, however, a considerable loss will occur in the stripline, increasing receiver noise temperatures. According to a theoretical analysis by De Lange *et al*<sup>1</sup>, to operate Nb-SIS mixers beyond the gap frequency a stripline used a highly conductive metal can reduce the loss in comparison with a Nb superconducting stripline because the metal has a lower surface resistance at frequencies above the Nb gap. It has also been demonstrated theoretically that the low-temperature DC conductivity of a normal metal film plays a key role in reducing RF loss in a metal stripline. The lower loss can be achieved if a metal film is in the extreme anomalous regime in which both the electron mean free path  $l_e$  in the metal and the film thickness  $d$  are much larger than the classical skin depth  $\delta_c$ .

The first experimental tests were performed by Van de Stadt *et al*<sup>2</sup> in Nb-SIS junctions with Al striplines in a 1 THz waveguide mixer. Similar experiments were later reported by Bin *et al*<sup>3</sup> in a quasi-optical mixer, who showed a considerably improved noise temperature at 1 THz, and also by Schaefer *et al*<sup>4</sup>.

In this paper we report the development of a fabrication process for Nb-SIS junctions integrated with Al tuning circuits. In particular, ultra-high vacuum (UHV) evaporation technique is applied for the fabrication of the stripline, leading to a pure Al film and to a low surface resistance because of the extreme anomalous limit. Together with employing an optimized optical coupling in a waveguide measurement setup, these devices have shown reduced noise temperatures at 1 THz. Details of the heterodyne measurements will be reported elsewhere at this symposium<sup>5</sup>.

## II. Characterization of Aluminium Films

To fabricate low noise Nb-SIS mixers with Al striplines, two essential questions need to be considered. The first question is what kind of Al films should be chosen for a stripline. In the extreme anomalous regime, where  $l_e \gg \delta_c$  and  $d \gg \delta_c$ , a low surface resistance  $R_s$  is expected and is given by  $\gamma(\omega^2 \mu_0^2 l_e / \sigma_{dc})^{1/3}$ , otherwise  $R_s$  is usually high<sup>6</sup>. Here  $\gamma$  is a constant of 0.325,  $\omega$  is the frequency,  $\mu_0$  is the permittivity in vacuum, and  $\sigma_{dc}$  is DC conductivity. It is important to note that in this regime for a given frequency  $R_s$  is determined only by the Fermi velocity  $v_F$  in the metal, but not by  $\sigma_{dc}$  because the ratio  $l_e / \sigma_{dc} \propto v_F^{-2}$  according to the Drude formula<sup>7</sup> for DC conductivity. For several metals such as Ag, Al, and Cu, at 1 THz  $R_s$  can be calculated using the expression together with the free electron concentration (or  $v_F$ ) data<sup>7</sup>. The values are 0.12, 0.095, and 0.11  $\Omega$  for Ag, Al and Cu,

respectively. The frequency dependence of  $R_s$  is given by  $R_s(1\text{THz})f^{2/3}$ , where  $f$  is in units of THz. We choose Al for the stripline because of its lower  $R_s$  and also because it happens to be compatible with the existing Nb technology.

To produce the film which is in the extreme anomalous regime we evaporate Al in a Varian UHV system with a base pressure  $2 \times 10^{-10}$  mbar. The major advantage of using UHV films in comparison with sputtered films is the long electron mean free path at 4.2 K as manifested by a higher residual resistance ratio (RRR)  $R_{300}/R_{4.2}$ , as illustrated in fig. 1. For an Al film of 150 nm evaporated on a  $\text{SiO}_2/\text{Si}$  substrate we found that RRR is 11, suggesting a  $l_e$  of 145 nm and a  $\sigma_{dc}$  of  $3.7 \times 10^8 \Omega^{-1}\text{m}^{-1}$  at 4.2 K. As a result, the ratio  $l_e/\delta_c$  is about 6 at 1 THz. Thus, the criterion of the extreme anomalous limit can be easily met. Another advantage of using the UHV technique is the smooth film surface, which is believed to be a result of a low evaporation rate ( $\sim 0.25$  nm/sec).

For comparison Fig. 1 also illustrates RRR and  $l_e$  for a sputtered Al film on a glass plate. It was prepared with a power density of  $2.19 \text{ W/cm}^2$  in a Nordiko 2000 sputter system, which has a base pressure of  $2 \times 10^{-7}$  mbar. In this case the sputtering rate is 0.7 nm/sec. We found the ratio  $l_e/\delta_c$  to be about 2 at 1 THz, suggesting that the film is marginally in the extreme anomalous limit. Furthermore, the surface of a sputtered Al film, especially deposited with a higher power, is presumably rough.

### III. Device Fabrication

The second question is how to marry the additional fabrication steps with an existing process for all Nb-SIS junctions. We fabricate Nb SIS junctions with Al striplines based on a selective niobium over-etch process (SNOEP) described by Dierichs *et al*<sup>8</sup>. Two new fabrication steps are introduced: adding two Al layers for bottom and top wiring layers, together with a layer of  $\text{SiO}_2$ , to form a stripline, and patterning Nb/ $\text{AlO}_x$ /Nb SIS junction by etching through the entire tri-layer. In contrast to the standard Nb-SIS fabrication, only the upper Nb layer is etched to form a top electrode. Fig. 2 illustrates our fabrication process schematically. We start with a 2 inches round and double-polished fused-quartz substrate, which has a thickness of 200  $\mu\text{m}$ . (a) a 20 nm Nb layer is sputtered and 150 nm Al is evaporated in the UHV system. (b) the Al bottom wire is patterned by applying a positive resist and wet etching in phosphoric acid. (c) A tri-layer of Nb-Al-Nb (100 nm, 6 nm, and 100 nm) is sputtered on the whole sample in the Nordiko. The oxide barrier  $\text{AlO}_x$  is formed in an oxygen environment in a load-lock after the deposition of the first Nb layer and Al. (d) junctions are defined by RIE etching of Nb top and bottom electrodes in a gas mixture of  $\text{CF}_4 + 3\% \text{O}_2$  and with a power density of  $75 \text{ mW/cm}^2$ , but the barrier of  $\text{AlO}_x$ -Al is etched by RF sputter etching in Ar gas with a pressure of 8 mTorr. A power density of  $1.3 \text{ W/cm}^2$  is used. To etch the Nb layers additional Nb monitor layers are used for visual end-point detection. The etching mask is SPR2-1.3 positive resist. In this step, a slightly over etching also removes the bottom 20 nm Nb, which is not covered by the Al layer. (e) Anodization is done to form an isolation layer. Then 250 nm  $\text{SiO}_2$  is deposited in another sputter system

and patterned by lift-off to form a dielectric layer for the stripline and also an electrical isolation between the bottom and top wires. (f) 200 nm Al is sputtered on the whole substrate. The top Al wire is defined again by wet-etching using a Nb layer as an etching mask. The latter was sputtered and patterned by lift-off. The Nb layers under the bottom Al wire and above the top wire are applied to reduce DC series resistances and are supposed to have no influence upon heterodyne measurements. Finally Au contact pads are defined.

Concerning the lithography process, there are two crucial steps. Firstly, the precise definition of a small junction with an area of  $1 \times 1 \mu\text{m}^2$  by photolithography is difficult. Due to the use of normal UV mode in our contacting mask-aligner the pattern transfer ends up with a circular-shape junction although the design is a square of  $1 \times 1 \mu\text{m}^2$  in the e-beam written mask. A SEM micrograph of a typical Nb SIS junction after removing the top Al wire is shown in Fig. 3. The central part is the Nb top electrode. The surrounding is  $\text{SiO}_2$ . The additional structure lying between is also  $\text{SiO}_2$  as a result of the lift-off, which will be discussed later. One can also see that the area is smaller than  $1 \mu\text{m}^2$ . The reduced junction area is due to the isotropic etching and also due to etching of both the top electrode and the bottom electrode, being twice the etching time for all Nb junctions. Secondly, the lift-off process for defining  $\text{SiO}_2$  does not work as ideal as one might hope. Fig. 4 shows a SEM micrograph of a test Nb SIS junction after the deposition of  $\text{SiO}_2$  (before the lift-off). As indicated in the figure, a  $\text{SiO}_2$  layer covers the photoresist entirely, making lift-off extremely difficult. This is the reason why there is the additional structure in Fig. 3. We explain the lift-off difficulty as a result of the sputtered  $\text{SiO}_2$ , which is isotropically deposited on the sample, but not the profile of the photoresist. The resist profile after the etching process of the tri-layer is illustrated in Fig. 5 and remains reasonably good.

#### IV. Results

A typical current-voltage ( $I$ - $V$ ) curve of Nb-SIS junctions with Al striplines is shown in Fig. 6, which is measured in a dipstick without filtering and screening of magnetic fields. Because of the use of additional Nb layers no series resistances are present in the  $I$ - $V$  curve. Typical DC properties of an Al stripline SIS junction, such as junction area  $A$ , normal state resistance  $R_n$ , current density  $J_c$ , gap voltage  $V_g$ , gap voltage spreading  $dV_g$ , ratio between the subgap resistance  $R_j$  and  $R_n$ , and  $\omega R_n C$  product, are summarized as follows:

Area:	$0.9 \mu\text{m}^2$
$R_n$ :	$30 \Omega$
$J_c$ :	$7 \text{ kA/cm}^2$
$V_g$ :	$2.8 \text{ mV}$
$dV_g$ :	$0.18 \text{ mV}$
$R_j/R_n$ :	20
$\omega R_n C$ :	13 (at 1 THz)

In the calculation of  $\omega R_n C$  the specific capacitance used is  $70 \text{ fF}/\mu\text{m}^2$ . Although additional Al layers are introduced, in comparison with our all Nb-SIS devices the quality in terms of  $I$ - $V$  characteristic is comparable.

Several devices have been tested in a 1 THz waveguide mixer block. At a measurement temperature of  $\geq 4.2 \text{ K}$ , best DSB noise temperatures of 700 K at 0.9 THz and 1000 K at 1 THz were obtained using a device with a  $48 \mu\text{m}$  long and  $10 \mu\text{m}$  wide end-loaded Al stripline. Also the upper-limit of the video response determined with a Fourier Transform Spectrometer in a device with a  $42 \mu\text{m}$  long and  $10 \mu\text{m}$  wide end-loaded Al stripline reaches as high as 1.1 THz, which is 1.6 times the gap frequency. In comparison with our previously reported results measured in Al stripline devices with thinner ( $\sim 80 \text{ nm}$ ) and less pure sputtered Al films<sup>2</sup>, these results are considerably improved concerning noise temperatures and the upper limit of RF response. In our experiment an optimization of optical coupling in the measurement setup, as described by Van de Stadt *et al*<sup>5</sup>, also plays an important role in the improvement. The noise temperatures we obtain are similar to those of a 1 THz quasi-optical Nb SIS mixer also with Al striplines reported by Bin *et al*<sup>3</sup>, who obtained at 1 THz DSB noise temperatures of 1170 K and 840 K at measurement temperatures of 4.2 K and 2.5 K, respectively.

## V. Discussions

The time for RF Ar sputter etching of an  $\text{AlO}_x$ -Al barrier is critical in our process. At present we use 7 min as etching time. An over-etching of 1~2 min can cause damage to the barrier, either resulting in a leaky  $I$ - $V$  characteristic or in increased subgap current. A typical  $I$ - $V$  curve of a junction with a damaged barrier is given in Fig. 7. An observed excess current in the  $I$ - $V$  characteristic for voltages beyond the gap is a signature of damaged barrier<sup>9</sup>. The damage is likely to occur around the edge of a SIS junction. To etch the barrier there are two alternative ways. One is RIE in a chlorine-containing gas, which is unfortunately not available in our laboratory. The other is RIE in  $\text{CF}_4$  gas with a lower pressure, but with a much higher power<sup>10</sup>.

Surface roughness of an Al film used for a stripline may have a significant influence on the surface resistance and thus mixer performance if the fluctuation in the surface has the same order of magnitude as the classical skin depth. Unfortunately to our knowledge there are very few experimental data available on this subject. To study the surface roughness, we have performed atomic force microscope (AFM) measurements on two Al films which were used in the experiment in Fig. 1, one being 150 nm UHV Al and the other being 200 nm sputtered Al film. Our preliminary results show surface roughness (peak-to-valley) of 10-15 nm for UHV Al and 40 nm for the sputtered Al, indicating that the UHV Al film has better surface morphology. Because the substrates are also different, these results remain inconclusive.

It is also important to realize that the physical properties of an Al surface such as roughness and purity may be modified in the fabrication process. This may be by a chemical

attack of the surface by, for example, photoresist developer, by the inter-diffusion between Al and Nb, and by radiation damage due to RIE.

Concerning the yield, we have so far not yet produced sufficient devices to establish a number. One batch of Al stripline devices showed a yield as high as 80 % in terms of  $I$ - $V$  curve and  $R_n$  value. In general we expect a lower yield than for all Nb-SIS devices because of the additional processing steps, such as etching through the barrier.

The post-process of dicing and polishing may further reduce the yield. It is required that for a 1 THz waveguide mixer the quartz substrate must be diced to as narrow as  $\sim 70$   $\mu\text{m}$  and polished to as thin as 40  $\mu\text{m}$ . We noticed that Al stripline devices are not as "strong" as all Nb-SIS junctions against both chemical and mechanical treatments.

The use of Al stripline can reduce DC heating effect in Nb junctions and particularly in NbN junctions<sup>11</sup>. Concerning the NbN mixers, using NbN SIS junctions in combination with Al striplines may also reduce the loss because high surface resistances are usually expected for poly-crystalline NbN films. The fabrication process described here is in principle also adequate for Al stripline NbN devices.

## **VI. Summary**

In summary we present a new fabrication process for Nb SIS junctions integrated with Al striplines. In particular, we have paid a careful attention to Al films for the stripline to obtain the surface resistance as low as possible. Heterodyne measurements using these devices show one of the lowest noise temperatures at 1 THz.

**ACKNOWLEDGMENT:** The authors would like to thank R.W. Stok for performing the AFM measurements and M. Mulder for his assistance in UHV evaporation. We acknowledge useful discussions with N. Whyborn and S. Shitov. We also thank P. R. Wesselius and M.W.M. de Graauw for their support and encouragement. This work is financially supported by the European Space Agency under contract No. 1153/95/NL/PB and the Stichting voor Technische Wetenschappen which is part of the Nederlandse Organisatie voor Wetenschappelijk Onderzoek.

## **References**

1. G. de Lange, J.J. Kuipers, T.M. Klapwijk, R.A. Panhuyzen, H. van de Stadt and M.W.M. de Graauw, *J. Appl. Phys.* **77**, 1795(1995)
2. H van de Stadt, A. Baryshev, P. Dieleman, M.W.M. de Graauw, T.M. Klapwijk, S. Kovtonyuk, G. de Lange, I. Lapitskaya, J. Mees, R.A. Panhuyzen, G. Prokopenko, and H. Schaeffer, *6<sup>th</sup> Int. Symposium on Space Terahertz Technology*, Pasadena, USA, March 1995, p.

3. M. Bin, M.C. Gaidis, J. Zmuidzinas, T.G. Phillips, and H. G. LeDuc, *Proc. of Int. Superconductive Electronics Conf.*, September 1995, Nagoya, Japan.
4. F. Schaefer *et al*, *Proc. of the 3rd Int. Workshop on THz Electr.*, Zermatt, 1995.
5. H. van de Stadt, A. Baryshev, J. R. Gao, H. Golstein, M.W.M. de Graauw, W. Hulshoff, S. Kovtonyuk, H. Schaeffer and N. Whyborn, in this conference.
6. G. E. H. Reuter and E.H. Sondheimer, *Proc. R. Soc. Ser. A* **195**, 33(1948).
7. C. Kittel, *Introduction to Solid State Physics*, 6<sup>th</sup> ed., Wiley and Sons.
8. M.M.T.M. Dierichs, R.A. Panhuyzen, C.E. Honingh, M.J.de Boer, and T.M. Klapwijk *Appl. Phys. Lett.* **2**, 774 (1993)
9. T.M. Klapwijk, *SQUID '85*, Berlin, 25-28 June, 1985, Eds. H.D. Hahlbohm and H. Luebbig, de Gruyter, p.1
10. D. Maier *et al*, private communications.
11. P. Dieleman, T.M. Klapwijk, S. Kovtonyuk, and H. van de Stadt, *Proc. of Applied Superconductivity*, Edinburgh, 3- July, 1995, edited by D. Dew-Hughes, 1995 IOP Published Ltd. p1315

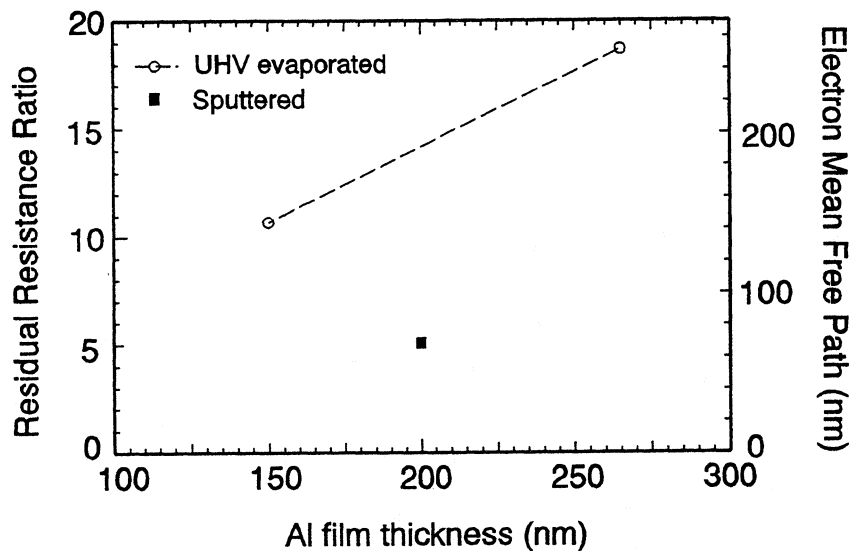


Figure 1. Residual resistance ratio between 300 K and 4.2 K (in the left hand) and electron mean free path (in the right hand) as a function of the thickness of Al films. Two types of the films, UHV evaporated Al on a SiO<sub>2</sub>/Si substrate and sputtered Al on a glass plate, are shown.



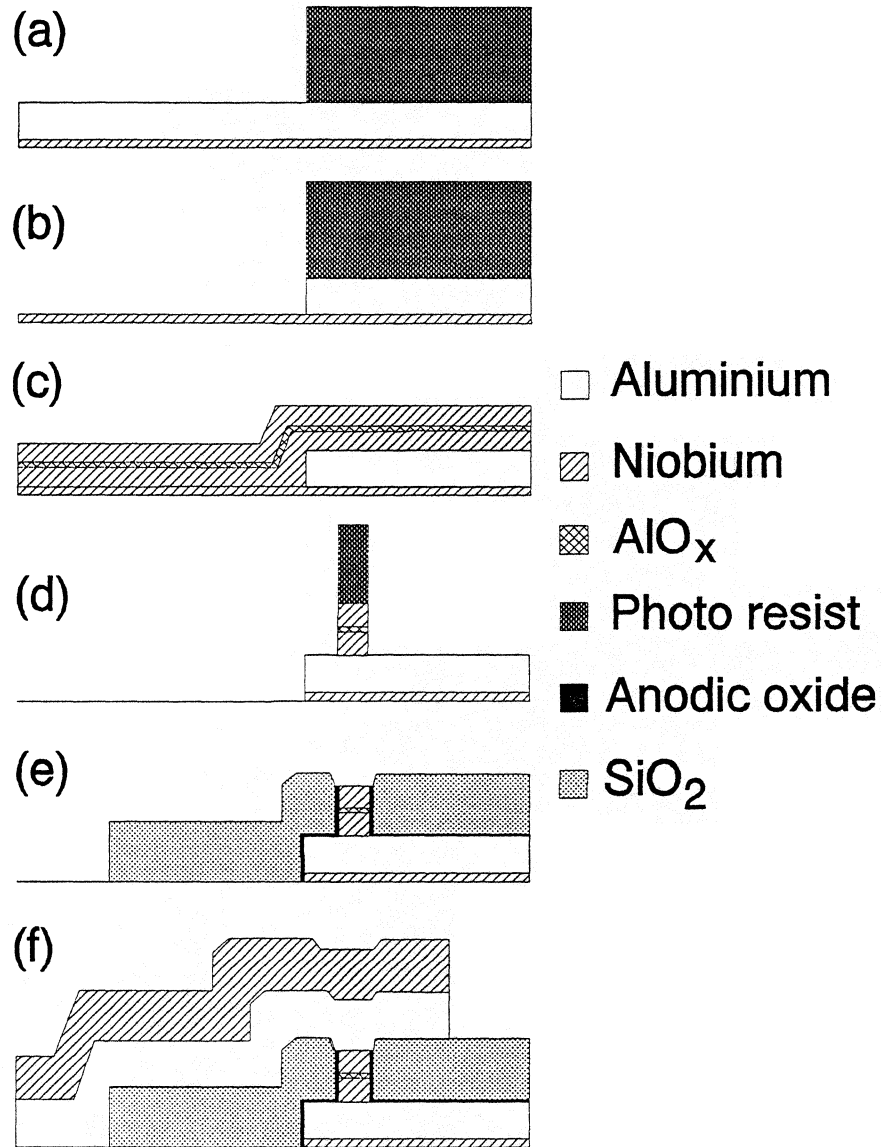


Figure 2. Fabrication flowing diagram for Nb SIS junctions with Al striplines.

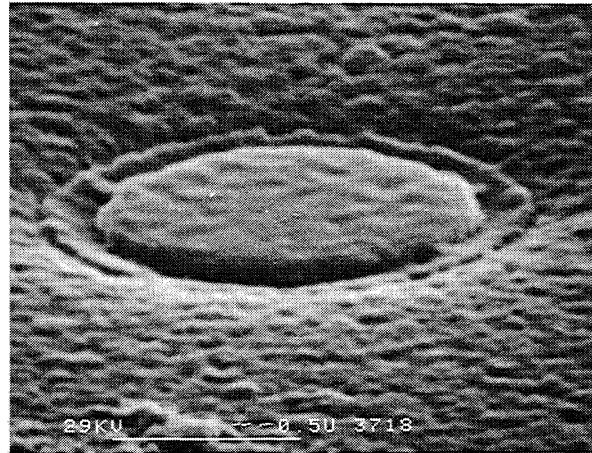


Figure 3. A SEM micrograph of a Nb SIS junction after removing the Al top wire, which is fabricated according to the process described in figure 2. The bar in the micrograph is 0.5  $\mu\text{m}$ .

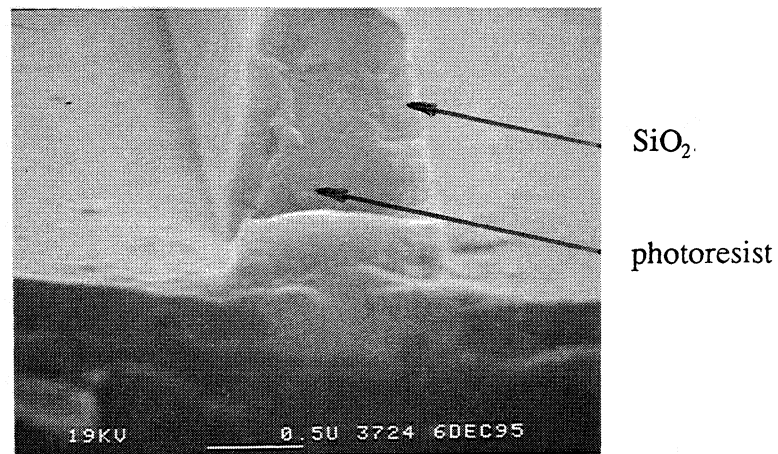


Figure 4. A cross-sectional SEM view of a test SIS junction after the deposition of SiO<sub>2</sub>. The structure shows the photoresist in the center. The resist is fully covered by SiO<sub>2</sub>. The bar in the micrograph is 0.5  $\mu\text{m}$ .

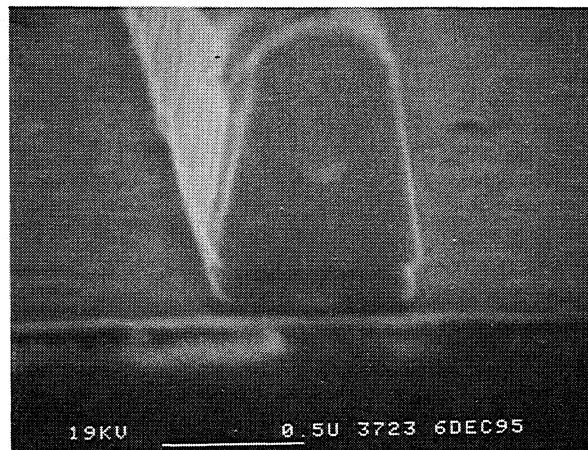


Figure 5. A SEM micrograph of a cross-sectional view of the photoresist and the tri-layer after the etching process for a test Nb junction. The bar in the micrograph is 0.5  $\mu\text{m}$ .

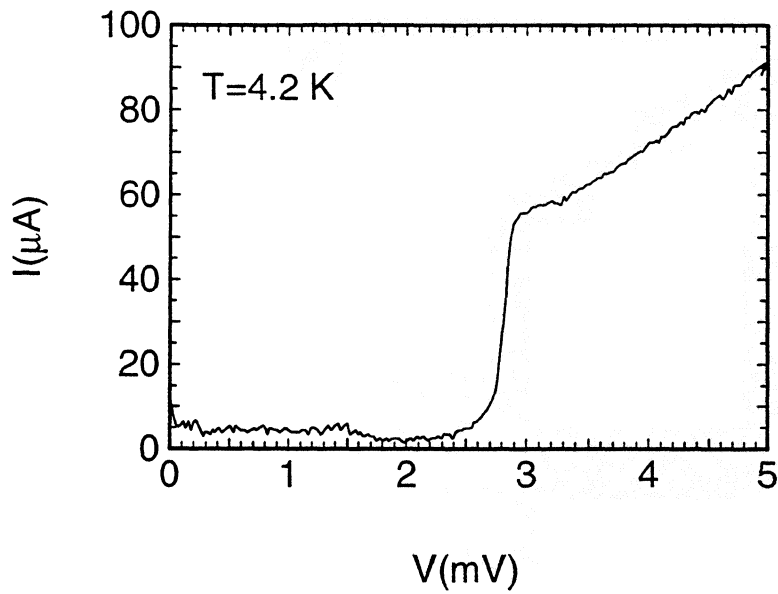


Figure 6. A typical current-voltage curve of  $\sim 1 \mu\text{m}^2$  Nb SIS junction with an Al stripline measured at 4.2 K.

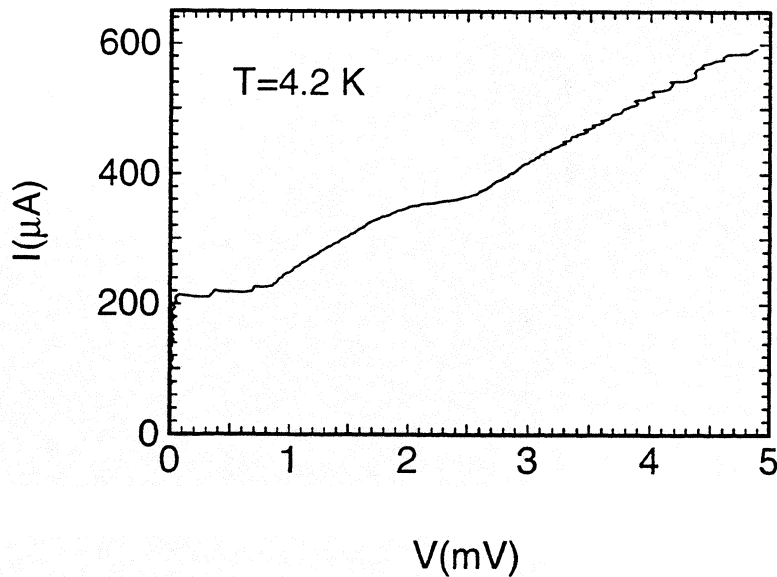


Figure 7. A typical current-voltage characteristic measured in a Nb SIS junction with a damaged barrier due to RF Ar sputter over-etching.